Available online at www.sciencedirect.com
ScienceDirect
Journal of Molecular Catalysis A: Chemical 264 (2007) 270–279
JOURNAL OF MOLECULAR CATALYSIS A: CHEMICAL
www.elsevier.com/locate/molcata

Effect of preparation technique on the properties of platinum in NaY zeolite: A study by FTIR spectroscopy of adsorbed CO

Kristina Chakarova [a], Konstantin Hadjiivanov [a,*], Genoveva Atanasova [a], Krassimir Tenchev [b]

[a] *Institute of General and Inorganic Chemistry, Bulgarian Academy of Sciences, Acad. G. Bonchev Street, Building 11, Sofia 1113, Bulgaria*
[b] *Institute of Catalysis, Bulgarian Academy of Sciences, Acad. G. Bonchev Street, Building 11, Sofia 1113, Bulgaria*

Received 8 August 2006; received in revised form 20 September 2006; accepted 21 September 2006
Available online 26 September 2006

Abstract

Two platinum-containing zeolites were studied by XPS, TPR and IR spectroscopy of adsorbed CO. The sample Pt–NaY was prepared by ion-exchange and the Pt/NaY sample, by impregnation. XP spectra indicate a higher heterogeneity of platinum on the impregnated sample and enrichment of its outer surface in platinum, compared to the exchanged sample. Accessible platinum in both activated samples is in the form of metal. However, oxidation of Pt–NaY with a $NO + O_2$ mixture results in creation of cationic sites. Adsorption of CO on the sample thus treated leads to formation of different platinum carbonyls: (i) $Pt^{3+}(CO)_2$ species (2204 and 2168 cm^{-1}) which are decomposed without production of monocarbonyls, (ii) two kinds of Pt^{2+}–CO species (2155 and 2141 cm^{-1}), (iii) $Pt^{+}(CO)_2$ dicarbonyls (2127 and 2091 cm^{-1}) and (iv) linear Pt^0–CO species (2080–2054 cm^{-1}). In contrast, almost no cationic sites were produced after the attempts to oxidize the impregnated sample. In both samples Chini-complexes were formed after interaction with CO at 373 K. However, the process was much easier with the impregnated sample. This indicates that exchanged cations, interacting more strongly with the zeolite matrix, are not suitable for preparation of anionic carbonyls. The effect of the preparation technique is discussed and the results are compared with the results on platinum in other zeolites.

Keywords: Adsorption; Carbon monoxide; FTIR spectroscopy; Chini-complexes; Platinum

1. Introduction

Although a plenty of studies are devoted to characterization of different platinum-containing catalysts, as a rule, the efforts have been concentrated on metal-containing samples, which in most cases, are the active catalysts [1–12]. Recently, it was indicated [13,14] that in some reactions the active sites could be platinum cations or Pt^{n+}/Pt^0 red–ox couples. To understand the mechanisms of these catalytic reactions and design new effective catalysts, it is important to know the state of the cations from the active phase. Characterisation of cationic platinum sites is also important for understanding the evolution of metal platinum catalysts. One of the most appropriate techniques for this purpose is infrared spectroscopy of probe molecules [1,15]. The most frequently used IR probe molecule is CO, which can provide information on the oxidation and coordination state of the coordinatively unsaturated surface cations and their Lewis acidities [1,15,16]. Although the carbonyl chemistry of platinum has been subject of a steady interest, the number of studies devoted to CO adsorption on non-reduced platinum catalysts is restricted [3,12–14,17–29]. It is generally accepted that surface carbonyls of cationic platinum are observed above 2100 cm^{-1}, but there is no consensus on the oxidation state of the adsorption sites. Very often the carbonyl bands at higher frequencies have been simply assigned to $Pt^{\delta+}$–CO species [3,12,20,23,30–32].

A series of difficulties associated with the use of CO as a probe can arise from the reductive properties of this molecule. Some transition metal cations react with CO, thus changing their oxidation state during the experiments [1,16]. Another complication with CO as a probe arises from the ability of many of the above cations to form the so-called *complex-specified* polycarbonyl species (that are decomposed without producing monocarbonyls). In particular, the situation with platinum in zeolites is even more complicated because of the willingness of platinum to form Chini-complexes, i.e. anionic platinum carbonyls [33–36].

* Corresponding author. Tel.: +359 2 9793598; fax: +359 2 705024.
E-mail address: kih@svr.igic.bas.bg (K. Hadjiivanov).

1381-1169/$ – see front matter © 2006 Elsevier B.V. All rights reserved.
doi:10.1016/j.molcata.2006.09.040

The aim of this work is to investigate the species produced after interaction of CO with Pt–NaY and Pt/NaY samples and to compare the results obtained with other platinum-containing systems.

2. Experimental

Two platinum containing Y zeolites were studied in this work: Pt–NaY, prepared by ion-exchange and Pt/NaY, synthesised by impregnation. The starting NaY material was supplied by Grace Davision (SP No. 6-5257.0101, Si/Al = 2.7).

The Pt–NaY sample was prepared by a conventional ion-exchange procedure. One gram of NaY was suspended in 10 mL 0.0157 M solution of $Pt(NH_3)_4Cl_2$ and stirred for 120 h at ambient temperature. Then the precipitate was thoroughly washed with distilled water and dried at 353 K for 8 h. The platinum concentration in the sample thus obtained was 3.06 wt%.

The Pt/NaY sample was prepared by impregnation. 1 gram of NaY was impregnated with 5 mL 0.0157 M solution of $Pt(NH_3)_4Cl_2$. After drying at 353 K the procedure was repeated. The nominal platinum concentration in this sample was 3.00 wt% Pt.

The IR spectra were recorded on a Nicolet Avatar 360 spectrometer by accumulation of 64 scans at a spectral resolution of 2 cm^{-1}. Self-supporting pellets (ca. 10–20 mg cm^{-2}) were prepared from the sample powder and treated directly in the purpose-made IR cells. The latter were connected to a vacuum-adsorption apparatus with a residual pressure below 10^{-3} Pa. Prior to the adsorption measurements, the samples were heated in fresh oxygen (20 kPa for 15 min) in steps of 50 up to 723 K (1 h at this temperature) and then evacuated for 1 h at 723 K.

Carbon monoxide (>99.997) was supplied by Linde AG. Nitrogen monoxide (>99.0) was purchased from Messer Greisheim GmbH. Before use, carbon monoxide and oxygen were passed through a liquid nitrogen trap.

Temperature programmed reduction (TPR) of the samples was carried out in the measurement cell of a differential scanning calorimeter DSC-111 (SETARAM) directly connected to a gas chromatograph. The experiments were performed with 10 vol% hydrogen in argon (20 mL min^{-1}) at a heating rate of 15 K min^{-1}. The TPR profiles were normalized for the same catalyst mass. Before the experiments, the samples were calcined for 1 h under air flow (25 mL min^{-1}) at 673 K.

The XPS spectra were taken by an ESCALAB Mk II (VG Scientific) apparatus with an aluminium anode ($h\nu$ = 1486.6 eV). The base pressure in the chamber was 10^{-7} Pa. The binding energy values were corrected using the C 1s level (285.0 eV) of the carbon contaminants on the surface. Element concentrations were evaluated from the integrated peak areas after linear background subtraction using theoretical cross-sections [37].

2.1. Initial characterization of the samples

In order to obtain more information, the samples were initially characterized by XPS and TPR. The main XPS signal for platinum is $4f_{7/2}$. In cases when this signal is masked by the peak of Al (73 eV), as is our case, a Pt $4d_{5/2}$ peak can be used [38].

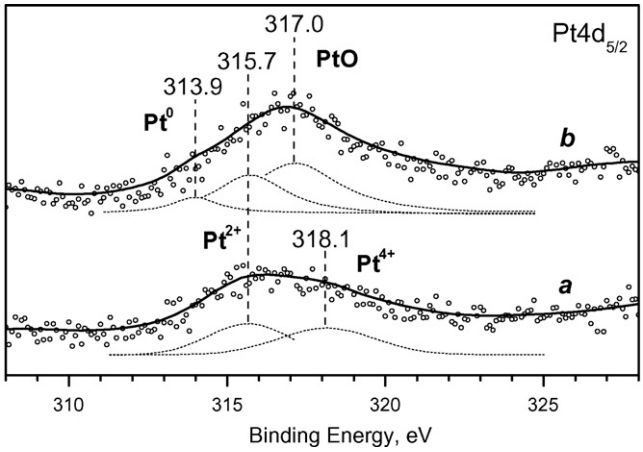

Fig. 1. XP spectra of ion-exchanged Pt–NaY (a) and impregnated Pt/NaY samples (b).

Generally, Pt^0 is characterized by a $4d_{5/2}$ peak at 313.9–314.4 eV. This signal shifts to higher binding energies with the increase of the platinum oxidation state and is detected at 314.9–317.1 and 317.9–318.4 eV for Pt^{2+} and Pt^{4+} ions, respectively. The photoelectron spectrum of the ion-exchanged Pt–NaY sample displays a complex band in the 310–325 eV region with maxima at 315.7 and 318.1 eV (Fig. 1, spectrum a). According to literature data [38–42], the main band at 315.7 eV is assigned to Pt^{2+} ions while the higher-energy shoulder is due to Pt^{4+} ions.

The XP spectrum of the impregnated Pt/NaY sample (Fig. 1, spectrum b) also contains a complex band with a distinguished maximum at 317.0 eV and two lower-energy shoulders at 315.7 and 313.9 eV (the exact positions of these shoulders were determined by a computer deconvolution of the spectrum and the peaks are presented by dotted lines). The main peak at 317.0 eV is typical of Pt^{2+} ions in PtO whereas the band at 315.7 eV, which was also detected in the spectrum of ion-exchanged sample, is due to isolated Pt^{2+} ions. The low intensity shoulder at 313.9 eV characterizes Pt^0. The above results show that platinum is less oxidized on the impregnated Pt/NaY than on the ion-exchanged sample.

The Pt:Si ratio, calculated on the basis of the XPS spectra, was 1:100 and 1.4:100 for the ion-exchanged (Pt–NaY) and impregnated (Pt/NaY) samples, respectively. This suggested that the external zeolite surface of Pt/NaY was enriched in platinum as compared to Pt–NaY.

The reducibility of the samples was established by TPR. Since the reduction temperatures depend on a series of factors such as preparation technique, calcinations temperature, support, etc., reduction peaks of platinum-containing catalysts are registered in a very wide temperature range, namely between 300 and 830 K [11,39,43–46]. The TPR profile of the calcined Pt–NaY sample contains one main peak with a maximum at 451 K (Fig. 2, pattern a). In addition, a series of low-intensity peaks at higher temperatures are detected. The main peak can be attributed to one-step reduction of oxidized platinum species to metal while the higher-temperature peaks could be due to reduction of platinum cations in less accessible positions.

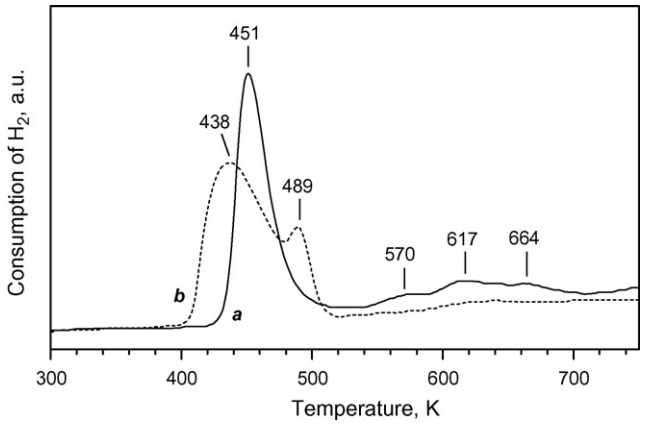

Fig. 2. TPR profiles of ion-exchanged Pt–NaY (a) and impregnated Pt/NaY samples (b).

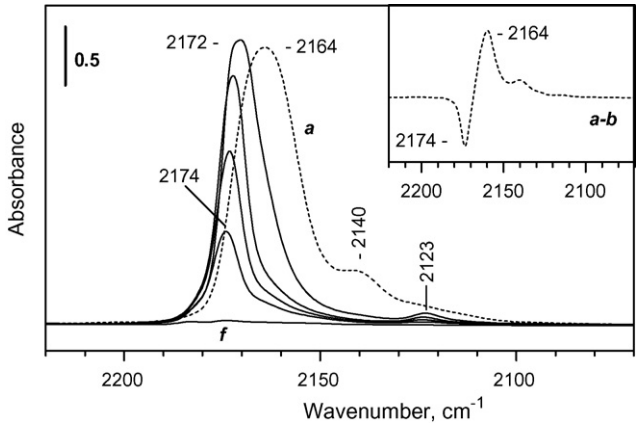

Fig. 3. FTIR spectra of CO (20 Pa equilibrium pressure) adsorbed at 100 K on NaY (a) and evolution of the spectra in dynamic vacuum at 100 K (b–f). The spectra are background corrected.

In the TPR profile of the impregnated Pt/NaY sample two peaks, at 438 and 489 K, respectively, are observed (Fig. 2, pattern b). The former peak is broad and more intense and is probably due to the reduction of the main part of platinum cations to Pt^0. Its maximum is situated at lower temperature than the corresponding reduction peak in the TPR profile of the ion-exchanged Pt–NaY which suggests easier reducibility of the impregnated sample. The weaker band at 489 K could also arise from less accessible platinum. These results evidence some heterogeneity of the Pt^{n+} ions in the Pt/NaY sample.

2.2. Background IR spectra of the samples

The IR spectrum of the activated NaY displays no bands in the O–H stretching region. On the contrary, the spectrum of the platinum supported samples, recorded after evacuation at 673 K, contains three bands at 3744, 3691 and 3648 cm^{-1} (spectra not shown). Since both the ion-exchange and the impregnation procedures are carried out in acid media, it is logical to expect the presence of protons in the samples thus prepared. The bands with maxima at 3744 and 3648 cm^{-1} are assigned to the O–H stretching modes of silanol groups and zeolite high-frequency (HF) hydroxyls, respectively [1,47,48]. The band at 3691 cm^{-1} is not observed with H_2-reduced samples and most probably characterizes Pt^{n+}–OH species.

At lower frequencies a series of bands in the 2000–1600 cm^{-1} region were detected. They were attributed to overtones and combinations of the zeolite skeletal vibrations [49]. These bands are of low intensity because of the low Si/Al ratio typical of zeolite Y. The self-absorption bands of the samples appear below ~1240 cm^{-1}, determining the 'cut-off' of the samples at this frequency.

2.3. Low-temperature adsorption of CO on NaY

To be able to distinguish between the carbonyl species formed with the participation of Pt and the support, respectively, it is necessary to know in details the species arising after CO adsorption of the support. The results on the same NaY sample were already published [50] and here we shall briefly recall the main observations.

CO adsorption at room temperature was negligible due to the lack of strong acid sites on the sample.

Adsorption of CO (20 Pa equilibrium pressure) at 100 K on activated NaY leads to the appearance of bands due to $Na^+(CO)_2$ species (2164 cm^{-1}) and physically adsorbed CO (2140 cm^{-1}) (Fig. 3, spectrum a). Evacuation at low temperatures provokes a quick disappearance of the latter band (Fig. 3, spectrum b). In parallel with this, the band at 2164 cm^{-1} is converted into a band at 2174 cm^{-1}, characterizing Na^+–CO species (see the inset in Fig. 3). At the same time, a weak band at 2123 cm^{-1} (resulting from the superposition of two bands due to ^{13}CO adsorbed on Na^+ sites and O-bonded CO, respectively) becomes visible. Further evacuation results in an additional shift of the Na^+–CO band at 2172–2174 cm^{-1} accompanied by a gradual reduction in its intensity (Fig. 3, spectra c–e) and ultimate disappearance (Fig. 3, spectrum f). In parallel with this, the low-intensity band at 2123 cm^{-1} also disappears.

2.4. Adsorption of CO on Pt–NaY

Adsorption of CO on an activated Pt–NaY sample leads to the appearance of a broad intense band at 2083 cm^{-1} with a lower-frequency shoulder at ~2100 cm^{-1} (spectra not shown). According to literature data [1,2,5,9,11,16,19,25,39,40,51], these two bands are assigned to linear Pt^0–CO complexes. Careful analysis of the spectra shows the presence of two other bands of a very low intensity, their maxima being at 2204 and 2168 cm^{-1}. They are due to carbonyl complexes formed with the participation of platinum cations. These results evidence an easy reducibility of Pt^{n+} ions even during the activation process.

In order to obtain more information on the cationic platinum carbonyls, we subjected the sample to oxidation treatment. It is well known that a $NO + O_2$ mixture is a stronger oxidizing agent than is oxygen itself. That is why we heated the sample in a NO (1 kPa partial pressure) + O_2 (7 kPa partial pressure) mixture at 673 K for 1 h and then evacuated the gas phase at the

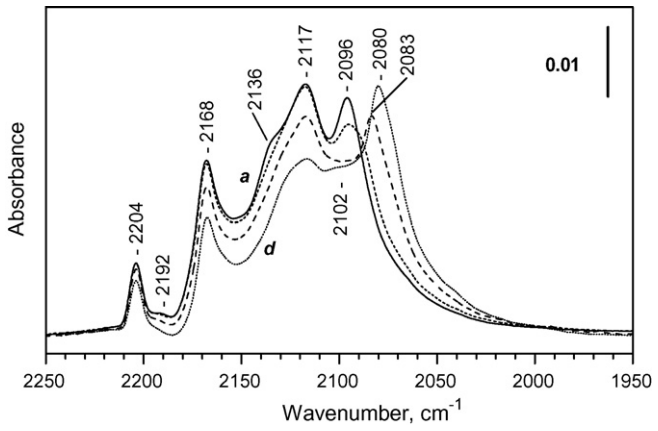

Fig. 4. FTIR spectra of CO (1 kPa equilibrium pressure) adsorbed at 298 K on oxidized Pt–NaY (for conditions see text) (a) and evolution of the spectra in dynamic vacuum at 298 K (b–d). The spectra are background corrected.

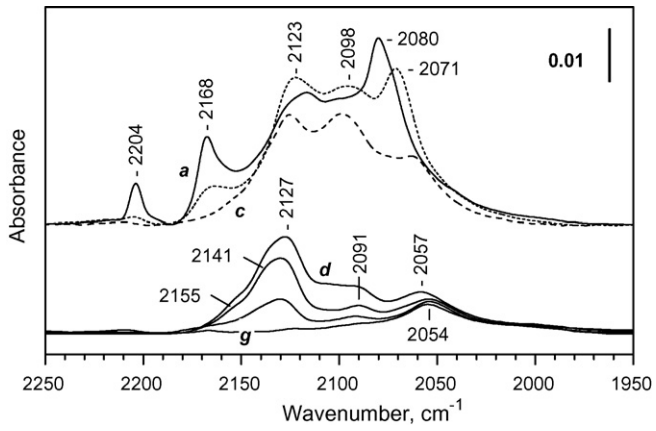

Fig. 5. Continuation of Fig. 4. FTIR spectra of CO (1 kPa equilibrium pressure) adsorbed at 298 K on oxidized Pt–NaY: evolution of the spectra in dynamic vacuum at 298 (a), 373 (b), 473 (c), 573 (d), 623 (e), 673 (f) and 723 K (g). The spectra are background corrected.

same temperature. Adsorption of CO (1 kPa equilibrium pressure) on the Pt–NaY sample thus treated leads to the appearance of a series of bands with maxima at 2204, 2168, 2136, 2117 and 2096 cm^{-1} (Fig. 4, spectrum a). A weak band around 2192 cm^{-1} is also visible. No bands assignable to CO_2 were detected which indicated that no measurable reduction of platinum occurred during the experiment. With the decrease of the CO equilibrium pressure, the band at 2136 cm^{-1} disappears first (Fig. 4, spectrum b). At the same time, the band at 2096 cm^{-1} decreases in intensity and its maximum is slowly shifted to lower frequencies. The intensities of the bands at 2191, 2168 and 2117 cm^{-1} are also reduced (Fig. 4, spectrum c). Simultaneously, a new band at 2083 cm^{-1} develops at the expense of the 2096 cm^{-1} band, which disappears. Further evacuation leads to a decrease in intensities of all bands except for that at 2083 cm^{-1} (Fig. 4, spectrum d). The latter increases in intensity and is additionally shifted to 2080 cm^{-1}. A new feature around 2102 cm^{-1} emerges in parallel with these changes.

Since the stable towards evacuation bands at 2204, 2168, 2117 and ∼2100 cm^{-1} were not detected with the pure support, they evidently characterized different platinum carbonyls. It was already mentioned that the bands around and below 2100 cm^{-1} were due to carbonyls of Pt^0 [1,2,5,9,11,16,19,25,39,40,51] whereas the higher-frequency bands were generally assigned to carbonyls of platinum cations [3,12,17–21,23–25,32,51–53]. Solomennikov and Davydov [3] reported the same bands at 2205 and 2175 cm^{-1} on a Pt–NaY sample and attributed them to two kinds of platinum monocarbonyls. However, careful analysis of the spectra shows that the bands with maxima at 2204 and 2168 cm^{-1} change in concert, this suggesting that they are due to one species. It is evident that the lower frequency band is more intense. Such an intensity ratio is typical of dicarbonyls. Bands with similar frequencies were observed recently with Pt–H–ZSM-5 [27,28] and Pt–Na–MOR [29] samples and assigned to $Pt^{3+}(CO)_2$ species. In addition, the dicarbonyl structure was confirmed by coadsorption of a ^{12}CO–^{13}CO isotopic mixture. By analogy with the other Pt-containing zeolite systems, we presume that the species, characterized by bands with maxima at 2204 and 2168 cm^{-1}, are $Pt^{3+}(CO)_2$ dicarbonyls.

The weak band around 2192 cm^{-1} could characterize the symmetric modes of another kind of $Pt^{3+}(CO)_2$ geminal species. Unfortunately, the corresponding antisymmetric modes (supposed to be around 2150 cm^{-1}) cannot be detected due to the superposition with other bands in the region. Similar dicarbonyl complexes characterized by a set of bands at 2195 and 2155 cm^{-1} have already been detected after CO adsorption on a Pt–H–ZSM-5 sample [27,28]. On the other hand, it is not excluded that the 2191 cm^{-1} band could arise from linear Pt^{3+}–CO species, the corresponding Pt^{3+} sites being not able to form dicarbonyls for steric reasons.

Evolution of the spectra after evacuation at higher temperatures is presented in Fig. 5. Evacuation at 373 K (Fig. 5, spectrum a) leads to a significant decrease in intensity of the bands, characterizing $Pt^{3+}(CO)_2$ dicarbonyls (2204 and 2168 cm^{-1}). In parallel with these changes, two new bands with maxima at 2123 and ∼2098 cm^{-1} develop. The band of Pt^0–CO carbonyls at 2082 cm^{-1} declines and is shifted to 2071 cm^{-1}.

Increase of the evacuation temperature up to 473 K (Fig. 5, spectrum c) results in complete disappearance of the set of bands at 2204 and 2168 cm^{-1} and decrease in intensities of the bands at 2123 and ∼2098 cm^{-1}. Simultaneously, the maximum of the band at 2123 cm^{-1} is blue shifted to 2127 cm^{-1}. The band at 2071 cm^{-1} (Pt^0–CO) decreases strongly in intensity and is shifted to lower frequencies.

Evacuation at 573 K leads to disappearance of all bands above 2155 cm^{-1} and the bands at 2127 and 2098 cm^{-1} go on decreasing (Fig. 5, spectrum d). After evacuation at higher temperatures (Fig. 5, spectrum e), the intensities of the latter two bands are additionally reduced and the broad feature around 2098 cm^{-1} is localized at 2091 cm^{-1}. At the same time, two new bands at 2155 and 2141 cm^{-1} become visible (the exact positions of these bands were determined by the second derivative of the spectrum). The band characterizing carbonyls of metal platinum is shifted to 2054 cm^{-1}.

Further increasing of the evacuation temperature leads to the progressive decrease in intensities of all bands (Fig. 5, spectrum f). The band at 2054 cm^{-1} (Pt^0–CO) is the only band that remains in the spectrum after evacuation at 723 K (Fig. 5, spectrum g).

The above results demonstrate that the $Pt^{3+}(CO)_2$ dicarbonyls are decomposed without producing a measurable fraction of linear Pt^{3+}–CO species, i.e. the diligand configuration is favoured. This allows us to classify the dicarbonyls of Pt^{3+} as *complex-specified* [1,54].

The bands with maxima at 2155 and 2141 cm^{-1} most probably characterize two types of linear Pt^{2+} carbonyls. Similar bands of Pt^{2+}–CO complexes were detected with Pt–H–ZSM-5 (2150 cm^{-1}) [27,28] and Pt–Na–MOR (2146 cm^{-1}) [29].

Bands at 2122 and 2092 cm^{-1} were observed with a Pt–H–ZSM-5 sample and, on the basis of ^{12}CO–^{13}CO coadsorption experiments, assigned to $Pt^{+}(CO)_2$ dicarbonyls [27,28]. Interestingly, in this case the band due to the symmetric modes was more intense than the band of the antisymmetric ones. This was explained by the big cationic radius of Pt^+ allowing a small angle between the two coadsorbed CO molecules. By analogy with the Pt–H–ZSM-5 sample [27,28], the bands at 2127 and 2091 cm^{-1}, which change in concert, are assigned to $Pt^{+}(CO)_2$ dicarbonyls. Since no linear species were produced as a result of their decomposition, these dicarbonyls, similarly to the $Pt^{3+}(CO)_2$ species, could be attributed to *complex-specified* geminal species. Analysis of the spectra shows that at higher CO coverages the bands at 2127 and 2091 cm^{-1} are of lower intensities, which suggests formation of tricarbonyls. Similar conversion of dicarbonyls into tricarbonyl complexes of Pt^+ was observed after CO adsorption on Pt–H–ZSM-5 [27,28]. Unfortunately, we cannot determine unambiguously the spectral features of these tricarbonyl species because of the superposition with other intense bands in the region.

2.5. Adsorption of CO on Pt/NaY

In this section we shall describe briefly only the main results obtained with the impregnated Pt/NaY sample. Adsorption of CO at room temperature on activated Pt/NaY led to the appearance of a band at 2084 cm^{-1} due to linear Pt^0–CO carbonyls only (spectra not shown). This picture is very similar to that registered with the ion-exchanged Pt–NaY. With the aim of obtaining information on the cationic platinum carbonyls, we oxidized the impregnated sample in a NO (1 kPa partial pressure) + O_2 (7 kPa partial pressure) mixture for 1 h at 673 K and then evacuated the gas phase at the same temperature. Then CO (5.7 kPa equilibrium pressure) was adsorbed at room temperature on the sample thus treated. As a result, two bands with maxima at ~2170 and 2058 cm^{-1} (not shown) developed in the spectrum. They were assigned to Na^+–CO species [1,50] and Pt^0–CO complexes [1,2,5,9,11,16,19,25,39,40,51], respectively. Since CO is a weak base, at room temperature it can be adsorbed on sites possessing strong Lewis acidity only. In order to obtain information on all sites, the temperature in the IR cell was decreased to 100 K. As a result, a strong $Na^{+}(CO)_2$ band appeared at 2167 cm^{-1} along with two other bands at 2140 cm^{-1} (physically adsorbed CO) and 2123 cm^{-1} (superposition of bands of Na^+–^{13}CO and O-bonded CO) (spectra not shown). All these bands have already been detected with the pure support (see Fig. 3). Evacuation at 100 K leads to a quick disappearance of the band of physically adsorbed CO (2140 cm^{-1}). At the same time, the band characterizing $Na^{+}(CO)_2$ dicarbonyls (2167 cm^{-1}) also disappears and a new band at 2174 cm^{-1} (Na^+–CO) emerges at its expense (Fig. 6, spectrum a). The band with a maximum at 2123 cm^{-1} also decreases in intensity.

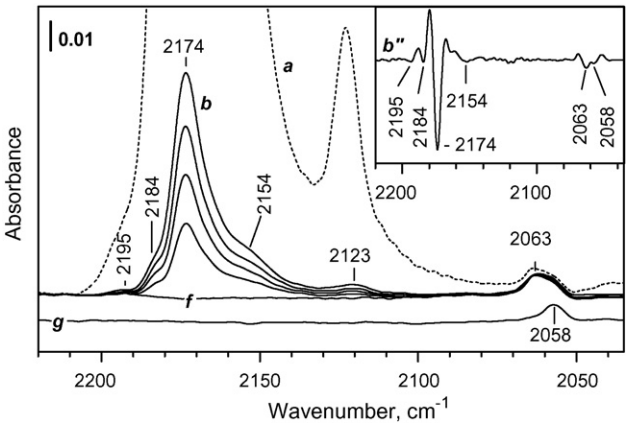

Fig. 6. FTIR spectra of CO (5.7 kPa equilibrium pressure) adsorbed at 100 K on oxidized Pt/NaY: evolution of the spectra in dynamic vacuum at 100 (a–f) and 298 K (g). The spectra are background corrected.

With the intensity decrease of the Na^+–CO band at 2174 cm^{-1}, some other bands become visible in the spectrum, their maxima being at 2195, 2184, 2154, 2063 and 2058 cm^{-1} (Fig. 6, spectrum b). Since these bands are of very low intensities and are seen as shoulders of the strong band at 2174 cm^{-1}, their exact positions were determined by the second derivatives (see the inset in Fig. 6). Further evacuation at 100 K leads to a gradual disappearance of all bands in the IR spectrum except for the two lowest-frequency bands at 2063 and 2058 cm^{-1} that remain unaffected (Fig. 6, spectra c–f). The latter band is the only one that remains in the spectrum after increasing the evacuation temperature to 298 K (Fig. 6, spectrum g).

The two bands with maxima at 2063 and 2058 cm^{-1} are assigned to Pt^0–CO species [1,3,12,17–21,23–25,32,36,51–53] while the higher-frequency bands characterize carbonyl complexes of platinum cations. The band at 2195 cm^{-1} is probably due to linear carbonyls of Pt^{3+} ions whereas the band with a maximum at 2154 cm^{-1} is assigned to Pt^{2+}–CO. Note that the bands of Pt^{n+}–CO species, appearing with the impregnated Pt/NaY sample, are of very low intensities and easily disappear during evacuation even at 100 K. On one hand, this can be explained by the fact that only a small amount of platinum in the impregnated sample is localized in cationic positions in the zeolite framework. On the other hand, it can be due, to some extent, to the more pronounced reducibility of the platinum cations in this sample. We were not able to detect any products of CO oxidation (CO_2, carbonate structures). This, however, could be due to the very low concentration of the cationic platinum species with this sample preparation.

2.6. Formation of anionic platinum carbonyls (Chini-complexes)

The Chini-complexes are anionic platinum carbonyls with the general formula $[Pt_3(CO)_6]_n^{2-}$. Such complexes have been produced after CO interaction with some Pt-containing zeolites having large pores, predominantly faujasites [33–36]. The formation of Chini-complexes requires a special treatment of inactivated samples in CO atmosphere at moderate temperatures (ca. 373 K). The rate of carbonylation is affected by the amount of zeolitic water. Water is assumed to play an important role, providing protons during the carbonylation process and helping in the migration of Pt species [36].

In order to produce Chini-complexes, the impregnated Pt/NaY sample was evacuated for 5 min at 333 K in vacuum (Fig. 7, spectrum a). This treatment was aimed at removing the air keeping some amount of zeolitic water. Under these conditions, two bands with maxima at 1641 and 1364 cm^{-1} were registered in the spectrum. The former band was due to the superposition of the H–O–H bending modes of water and the antisymmetric H–N–H deformations of the NH_3 ligands whereas the band at 1364 cm^{-1} characterized the symmetric H–N–H deformation modes of coordinatively bonded ammonia [16,35]. After that CO (19.3 kPa equilibrium pressure) was introduced into the cell and the sample was heated at 373 K under CO for 18 h. As a result, 1 h later two bands with maxima at 2058 and 1798 cm^{-1} appeared in the spectrum (Fig. 7, spectrum b). Simultaneously, the $\delta_s(NH_3)$ band at 1364 cm^{-1} started to lose intensity and a new band with a maximum at 1454 cm^{-1} developed at its expense. The band at 1641 cm^{-1} also increased in intensity. All these changes were more pronounced during the second hour after the reaction start (Fig. 7, spectrum c). Allowing the sample to stay for 18 h under CO at 373 K resulted in a strong increase in intensities of the bands at 2058 and 1798 cm^{-1}, their maxima being shifted to 2057 and 1810 cm^{-1}, respectively (Fig. 7, spectrum d). In parallel with this, the band at 1364 cm^{-1} was completely converted into the 1454 cm^{-1} band (settled at 1449 cm^{-1}). The latter was assigned to NH_4^+ [16,35]. Additionally, two weak bands at 1905 and 1864 cm^{-1}, attributed to bridged Pt^0–(CO)–Pt^0 carbonyls [2,25,51,53], emerged in the spectrum. A weak band at 2356 cm^{-1} was also discernible and assigned to adsorbed CO_2. It evidenced reduction of cationic platinum.

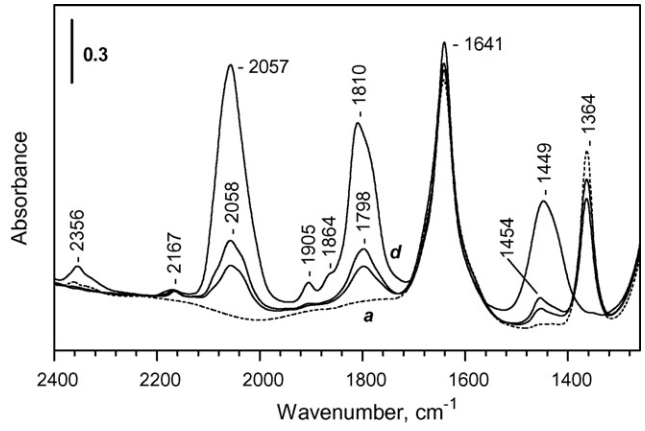

Fig. 7. FTIR spectra of impregnated Pt/NaY sample after evacuation for 5 min at 333 K (a) and after heating at 373 K in CO (19.3 kPa) for 1 (b), 2 (c) and 18 h (d).

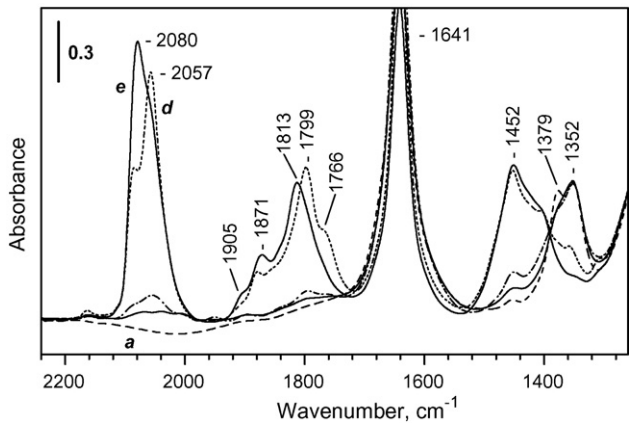

Fig. 8. FTIR spectra of ion-exchanged Pt–NaY sample after evacuation for 5 min at 333 K (a) and after heating at 373 K in CO (19.3 kPa) for 1 (b), 14 (c), 15 (d) and 18 h (e).

According to literature data [1,34–36], the two changing-in-concert bands at 2058 and 1798 cm^{-1} (shifted with time to 2057 and 1810 cm^{-1}, respectively) were assigned to Chini-complexes $[Pt_3(CO)_6]_n^{2-}$. The former band was due to linearly coordinated CO and the latter, to bridging CO.

Similar bands, indicating formation of Chini-complexes, were also observed with the ion-exchanged Pt–NaY sample (see Fig. 8). Besides, an interesting phenomenon was established, namely a strong dependence of the carbonylation rate on the preparation technique. In contrast to the results obtained with the impregnated sample, it was found that no measurable fraction of Chini-complexes was produced after one-hour heating of the ion-exchanged Pt–NaY in CO at 373 K (Fig. 8, spectrum b). Formation of $[Pt_3(CO)_6]_n^{2-}$ species was hardly observed until 14 h since the reaction starts (Fig. 8, spectrum c). During the next hour (Fig. 8, spectrum d) the bands at 2057 and 1799 cm^{-1}, characterizing the Chini-complexes, strongly increased in inten-

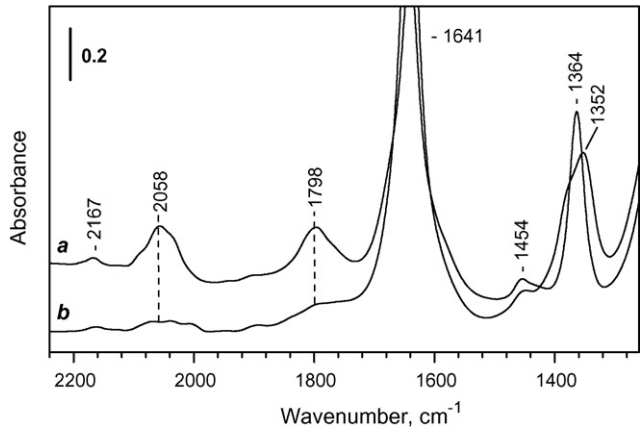

Fig. 9. FTIR spectra of impregnated Pt/NaY (a) and ion-exchanged Pt–NaY samples (b) after heating at 373 K in CO (19.3 kPa) for 1 h.

sities. At the same time, linear Pt^0–CO (2086 cm^{-1}) and bridged Pt^0–(CO)–Pt^0 (1877 cm^{-1}) carbonyl species were produced. Further stay of the sample in a CO atmosphere at 373 K (Fig. 8, spectrum e) led to additional increase in intensities of the latter two bands accompanied by a shift to lower frequencies of their maxima. The difference in the carbonylation rates is more clearly seen in Fig. 9 presenting the spectra obtained with impregnated and ion-exchanged samples after 1-h heating at 373 K in CO atmosphere.

3. Discussion

In this section we will not only discuss the results observed with the Pt–NaY and Pt/NaY samples, but, following our previous results obtained with other Pt-containing systems [27–29,55], will try to summarize the effect of the support on the oxidation and coordination state of deposited Pt^{n+} ions.

3.1. Effect of the support type on the oxidation state of platinum

The most typical oxidation states of platinum are 2+ and 4+, but compounds of Pt^{6+}, Pt^{5+}, Pt^{3+} and Pt^{+} are also known [56,57]. In addition, under special conditions, in the so-called Chini-complexes, platinum possesses a formal negative charge [1,33–36]. As mentioned above, there are hundreds of studies on CO adsorption over metallic platinum but very little attention has been paid to carbonyls formed with the participation of cationic platinum sites. The complexes formed after CO adsorption on the Pt^{n+} ions in different zeolites are summarized in Table 1. Our results indicate that the oxidation state of the supported platinum is rather dependant on the preparation technique and the preliminary treatments than on the support type. It was established that platinum in activated Pt–H–ZSM-5 [27,28] and Pt–Na–MOR [29] samples, as well as on the oxidized Pt–NaY, was mainly in the form of Pt^{3+} and/or Pt^{4+} ions. Supported Pt^{4+} ions are coordinatively saturated and not able to form carbonyls after CO adsorption. In the presence of CO, the Pt^{3+} sites are easily reduced but recovered after re-oxidation of the samples in a $NO + O_2$ mixture. It has to be noted that the easiest reduction of the Pt^{n+} cations has been observed in zeolite NaY. Adsorption of CO on activated Pt–NaY and Pt/NaY samples leads to the appearance of bands of Pt^0–CO carbonyls only (~2100 and 2083 cm^{-1}), which indicates auto-reduction of the Pt^{n+} ions even during the activation [58].

Additional information on the reducibility of the platinum cations in H–ZSM-5 and NaY was obtained by TPR. In brief, the TPR profiles of Pt–NaY and Pt/NaY show one-step reduction of the oxidized platinum species to Pt^0, which confirms the easy reduction of the Pt^{n+} ions in these samples. On the contrary, with ion-exchanged Pt–H–ZSM-5 and impregnated Pt/H–ZSM-5 samples two-step ($Pt^{4+} + Pt^{3+} + Pt^{2+}$) → Pt^{+} → Pt^0 reduction was found. Moreover, a dependence of the reduction temperature on the preparation technique was established with both zeolites. The maxima of the TPR peaks of impregnated samples are situated at lower temperatures than are the corresponding reduction peaks in the TPR profiles of the ion-exchanged samples, which suggests easier reduction of the platinum cations supported by impregnation.

3.2. Effect of the support type on the coordination state of Pt^{n+} ions

In contrast to the negligible effect of the support type on the oxidation state of platinum, it was found that the support was decisive for the coordination state of the Pt^{n+} cations whatever their oxidation states were. Generally, charge-compensating metal ions in zeolites have higher degrees of unsaturation than in the case of oxide-supported cations [1,59]. The structure of the oxide surfaces strongly depends on the preparation technique but, as a rule, the cations of the supported phase are characterized by one effective coordination vacancy. According to the above statement, only linear carbonyls of Pt^{n+} ions have been observed with oxide-supported samples [17,19,55].

In most cases cations in zeolites are 3-coordinated but, depending on their position could be 6- or 4-coordinated. According to literature data [60,61], three main cationic positions, S_I, S_{II} and S_{III}, could be distinguished in faujasites (X, Y zeolites). The S_I sites are favourable but cations in these positions are not accessible to CO adsorption. Preferable location of uni- and divalent cations are the S_{II} sites. In these positions the cations are 3-coordinated and possess three coordination

Table 1
Carbonyl complexes of Pt^{n+} ions in zeolites

	Pt–H–ZSM–5 [27,28]	Pt–Na–MOR [29]	Pt–NaY (this work)
Pt^{3+}	Two types $Pt^{3+}(CO)_2$ at 2211 and 2175 cm^{-1} and at 2195 and 2155 cm^{-1}	$Pt^{3+}(CO)_2$ at 2205 and 2167 cm^{-1}; less stable than the species in Pt–H–ZSM-5	$Pt^{3+}(CO)_2$ at 2204 and 2168 cm^{-1}; less stable than the species in Pt–H–ZSM-5
Pt^{2+}	$Pt^{2+}(CO)_2$ at 2165 and 2150 cm^{-1} Pt^{2+}–CO at ~2155 cm^{-1}	Pt^{2+}–CO at 2146 cm^{-1}	Two types Pt^{2+}–CO at 2155 cm^{-1} and at 2141 cm^{-1}
Pt^{+}	$Pt^{+}(CO)_3$ at 2162, 2150 and 2110 cm^{-1} $Pt^{+}(CO)_2$ at 2120 and 2091 cm^{-1} Pt^{+}–CO at 2113 cm^{-1}	$Pt^{+}(CO)_2$ at 2135 and 2101 cm^{-1} Pt^{+}–CO at 2111 cm^{-1}	$Pt^{+}(CO)_2$ at 2127 and 2091 cm^{-1}; at higher CO coverages probably converted into $Pt^{+}(CO)_3$
Pt^0	Pt^0–CO below 2100 cm^1	Pt^0–CO below 2102 cm^{-1} Pt^0–(CO)–Pt^0 at 1870 cm^{-1}	Pt^0–CO below 2096 cm^{-1} Pt^0–(CO)–Pt^0 at 1905–1871 cm^{-1}
Pt^{n-}	Not formed	Not formed	Chini-complexes $[Pt_3(CO)_6]_n^{2-}$ at 2057 and 1810 cm^{-1}

vacancies. It is found that the location of platinum cations in zeolite NaY depends on the preliminary treatment of the samples. When the samples are activated in oxygen atmosphere, the $Pt(NH_3)_4^{2+}$ complexes are decomposed, producing Pt^{2+} ions and ammonia [58]. XRD analysis has shown that when the activation temperatures are below 573 K, no Pt^{2+} cations are found in S_I, $S_{I'}$ and $S_{II'}$ sites. In this case Pt^{2+} cations, in form of PtO, are supposed to be localized into the supercages of the zeolite framework. Activation of the samples at temperatures above 673 K leads to migration of Pt^{2+} ions (produced as a result of interaction between PtO and the protons) from the supercages to the sodalite cages. On the basis of XRD data it is proven that after activation of the sample in oxygen atmosphere at 873 K, all Pt^{2+} ions are situated in $S_{I'}$ positions and are coordinated to three oxygen atoms [58]. When the platinum concentration is high enough after filling all $S_{I'}$ sites, the Pt^{n+} ions could occupy other positions, for instance the accessible to adsorption S_{II} sites. Our own results confirm this suggestion. Investigating another ion-exchanged Pt–NaY sample with platinum concentration of 1.00 wt% Pt (for brevity the results are not described here) we detected no platinum carbonyls after CO adsorption. This could be explained assuming that, because of their low concentration, Pt^{n+} ions occupy S_I positions only and are inaccessible to CO adsorption.

Bands of CO adsorbed on cationic platinum sites were registered with the 3% Pt–NaY sample. However, the intensities of these bands were lower than the intensities of the corresponding bands, detected with Pt–H–ZSM-5 [27,28] and Pt–Na–MOR samples [29], which indicates that even in this sample only a small part of the platinum cations occupy accessible positions in zeolite NaY.

Let us now discuss the different cationic platinum carbonyls formed in zeolites. It is evident from Table 1 that when the Pt^{3+} ions are exchanged in zeolites they produce dicarbonyl complexes. The $Pt^{3+}(CO)_2$ dicarbonyls belong to the so-called *complex-specified* dicarbonyls [1,54], i.e., they are decomposed without producing linear Pt^{3+}–CO species. It is believed that the *complex-specified* geminal species are produced because of reaching a stable electron configuration whatever the support is. However, dicarbonyls of Pt^{3+} ions were not detected after CO adsorption on oxide-supported samples [17,19,55], which evidences that in some cases these species are not produced for steric reasons. The stability of the $Pt^{3+}(CO)_2$ dicarbonyls registered in the Pt–NaY sample is similar to the stability of the corresponding species in Pt–Na–MOR [29] and lower than that in Pt–H–ZSM-5 [27,28]. In the latter case, the dicarbonyls are still observed after evacuation at 473 K, whereas in Pt–NaY and Pt–Na–MOR they are decomposed at this temperature. Furthermore, with Pt–NaY and Pt–Na–MOR samples the IR bands are at frequencies lower by 6–7 cm^{-1} than those detected with Pt–H–ZSM-5 (2211 and 2175 cm^{-1}). All this can be explained by a weaker σ-bonding when the $Pt^{3+}(CO)_2$ dicarbonyls are formed in the latter two samples. Hence, the Pt^{3+} cations are more electrophilic in a ZSM-5 matrix as compared to MOR and Y [59].

The Pt^{2+} ions in Pt–H–ZSM-5 also produced dicarbonyl species. Note that in this case the dicarbonyls are *site-specified*. Formation of the *site-specified* polycarbonyls is determined by the high degree of coordinative unsaturation of the cation and they are decomposed *via* production of monocarbonyls [54]. Indeed, it was found that the ability of a cation in exchanged position to coordinate more than one molecule depended on its cationic radius [62–64]. Small cations penetrate the oxygen ring where they are coordinated and, for steric reasons, can accept one guest molecule only. The critical cationic radius depends on the dimension of the O-rings and is, therefore, different not only for the different zeolites but also for the different cationic positions in one zeolite [63]. Since the O-rings in MOR are larger than those in ZSM-5, it is easy to explain why the Pt^{2+} ions in Pt–Na–MOR are not able to coordinate a second CO molecule [29] (see Table 1). Evidently, the Pt^{2+} ions are too small to form dicarbonyls in Pt–Na–MOR. Because of the strong superposition of bands in the spectra registered with the Pt–NaY, conclusions about the possibility of the Pt^{2+} cations in this sample to produce dicarbonyls cannot be made.

The Pt^{+} ions in Pt–H–ZSM-5 [27,28] and Pt–NaY form tricarbonyls which easily loose one CO ligand even at room temperature, being thus converted to $Pt^{+}(CO)_2$ dicarbonyls (see Table 1). The latter are thermally decomposed without producing linear species and, similarly to the dicarbonyls of Pt^{3+}, are classified as *complex-specified*. The Pt^{+} ions in Pt–Na–MOR form *site-specified* dicarbonyls only [29]. These results are in general agreement with the results observed with the Pt^{2+} cations. Since the decrease in oxidation state results in an increase of the cationic radius, it is logical to expect that the Pt^{+} cations in Pt–Na–MOR will be able to absorb two CO molecules each. However, the cationic radius of Pt^{+} seems to be not big enough for simultaneous adsorption of three CO molecules when the cations are exchanged in MOR in contrast to the case when they are in Pt–H–ZSM-5.

It is noteworthy that the antisymmetric modes of the $Pt^{+}(CO)_2$ dicarbonyls in Pt–H–ZSM-5 and Pt–NaY are less intense than the corresponding symmetric modes. This ratio is not typical of the dicarbonyl complexes. Usually, the angle between the CO ligands in surface dicarbonyls is bigger than 90° and the symmetric modes are less intense. However, in our case this angle is less than 90°. This phenomenon can be explained by the big cationic radius of Pt^{+} allowing a smaller angle between the ligands without steric hindrance.

The fact that after deposition $Pt(NH_3)_4^{2+}$ complexes are located in the supercages of the zeolite framework explains the ability of formation of Chini-complexes. Since these species are relatively big, they could only be produced with zeolites having a large pore size. Indeed, no Chini-complexes were produced with Pt–H–ZSM-5 and Pt–Na–MOR sample (see Table 1). The dimensions of the cavities in faujasite-type zeolites allow formation of complexes with 2–4 layers containing 6–12 Pt atoms [1]. Chini-complexes were produced with both ion-exchanged Pt–NaY and impregnated Pt/NaY samples but with a significant difference in the carbonylation rates. The results obtained suggest that platinum in the ion-exchanged sample is more strongly bound to the zeolite matrix, which impedes the formation of Chini-complexes.

3.3. Effect of the preparation technique on the state of Pt^{n+} ions

The results of this study imply that the preparation technique, ion-exchange or impregnation, strongly affect the state of platinum supported on the zeolite NaY. The two samples showed a significant difference in carbonylation rates during the formation of Chini-complexes and the carbonylation process is favoured with the impregnated Pt/NaY sample. On the other hand, cationic platinum carbonyls were produced much more easily with the ion-exchanged Pt–NaY sample. Note that carbonyl complexes of Pt^{n+} ions were hardly registered with the impregnated Pt/NaY sample even after low temperature CO adsorption. This could be due to the easier reducibility of the Pt^{n+} ions in this sample and the fact that only a small amount of platinum is located in cationic positions in the zeolite.

In contrast to the zeolite NaY, it was established that the preparation technique (ion-exchange or impregnation) hardly affected the state of platinum in H–ZSM-5 [27,28]. In this case, only a small amount of platinum cations being not in exchanged positions were found with the impregnated sample. This phenomenon can be explained by the different charge-compensating cations in the two zeolites. When the H-form of the zeolite is used, the protons are easy replaced by metal cations and even when platinum is supported by impregnation, the main part of it occupies cationic positions. On the contrary, when the Na-form of the zeolite is used as a support, the Na^+ cations remains in their position when impregnation is used to deposit platinum and most of the Pt^{n+} ions are not localized in cationic positions.

4. Conclusions

Adsorption of CO on an activated ion-exchanged Pt–NaY sample leads mainly to formation of carbonyls of Pt^0, which suggests auto-reduction of platinum cations during the activation process. After oxidation of the sample in a $NO + O_2$ mixture, various carbonyls, involving platinum cations in different oxidation states, were registered:

- $Pt^{3+}(CO)_2$ dicarbonyls (ν_s at 2204 cm^{-1} and ν_{as} at 2168 cm^{-1}) that are decomposed without producing linear species.
- Two types of Pt^{2+}–CO species (2155 and 2141 cm^{-1}). Unfortunately, because of the complexity of the spectra registered with the Pt–NaY sample, we are not able to make unambiguous conclusions about the possibility of the Pt^{2+} cations to form dicarbonyls.
- $Pt^{+}(CO)_2$ dicarbonyls (ν_s at 2127 cm^{-1} and ν_{as} at 2091 cm^{-1}) which do not produce monocarbonyls during decomposition. Most probably, at higher CO coverages the $Pt^{+}(CO)_2$ species are converted into tricarbonyls.

With the impregnated Pt/NaY sample carbonyls of platinum cations (in negligible amounts) were registered after CO adsorption at low temperatures only.

Anionic platinum carbonyls (Chini-complexes) were produced with both ion-exchanged Pt–NaY and impregnated Pt/NaY samples but with a significant difference in the reaction kinetics dependent on a different localization of Pt^{n+} cations in the zeolite framework after deposition by ion-exchange and impregnation, respectively, which determine a different bond strength with the zeolite matrix.

The preparation technique (ion-exchange or impregnation) strongly affects the state of platinum in zeolite NaY. A significant amount of platinum cations not in exchanged positions was found with the impregnated sample.

Acknowledgement

The authors are indebted to the Alexander von Humboldt Foundation for the support.

References

[1] K. Hadjiivanov, G. Vayssilov, Adv. Catal. 47 (2002) 307–511.
[2] P. Hollins, Surf. Sci. Rep. 16 (1992) 51–94.
[3] A. Solomennikov, A. Davydov, Kinet. Catal. 25 (1984) 403–407.
[4] A. Bourane, O. Dulaurent, K. Chandes, D. Bianchi, Appl. Catal. A 214 (2001) 193–202.
[5] P.C. Welch, P.S.W. Mills, C. Mason, P. Hollins, J. Electron Spectrosc. Relat. Phenom. 64/65 (1993) 151–154.
[6] J.A. Anderson, F.K. Chong, C.H. Rochester, J. Mol. Catal. A 140 (1999) 65–80.
[7] F. Gracia, W. Li, E.E. Wolf, Catal. Lett. 91 (2003) 235–242.
[8] A.M. Venezia, L. Liotta, G. Deganello, P. Terreros, M. Peña, J.L.G. Fierro, Langmuir 15 (1999) 1176–1181.
[9] M. Crocoll, S. Kureti, W. Weisweiler, J. Catal. 229 (2005) 480–489.
[10] T.N. Vu, J. van Gestel, J.P. Gilson, C. Collet, J.P. Dath, J.C. Duchet, J. Catal. 231 (2005) 453–467.
[11] L.R. Raddi de Araujo, M. Schmal, Appl. Catal. A 235 (2002) 139–147.
[12] Y. Yamasaki, M. Matsuoka, M. Anpo, Catal. Lett. 91 (2003) 111–113.
[13] W. Schiesser, H. Vinek, A. Jentys, Catal. Lett. 73 (2001) 67–72.
[14] R. Burch, J.A. Sullivan, J. Catal. 182 (1999) 489–496.
[15] H. Knözinger, in: G. Ertl, H. Knözinger, J. Weitkamp (Eds.), Handbook of Heterogeneous Catalysis, vol. 2, Wiley–VCH, Weinheim, 1997, p. 707.
[16] A. Davydov, Molecular Spectroscopy of Oxide Catalyst Surfaces, Willey, Chichester, 2003.
[17] K. Hadjiivanov, J. Chem. Soc., Faraday Trans. 94 (1998) 1901–1904.
[18] E. Shpiro, O. Tkachenko, N. Jaeger, G. Ekloff, W. Grunert, J. Phys. Chem. B 102 (1998) 3798–3805.
[19] K. Hadjiivanov, J. Saint-Just, M. Che, J.M. Tatibouet, J. Lamotte, J.-C. Lavalley, J. Chem. Soc., Faraday Trans. 90 (1994) 2277–2281.
[20] A. Stakheev, E. Shpiro, O. Tkachenko, N. Jaeger, J. Schulz-Ekloff, J. Catal. 169 (1997) 382–388.
[21] L. Marchese, M.R. Boccuci, S. Coluccia, S. Lavagnino, A. Zecchina, L. Bonneviot, M. Che, Stud. Surf. Sci. Catal. 48 (1989) 653–663.
[22] M. Primet, J.M. Basset, M.V. Mathieu, M. Prettre, J. Catal. 29 (1973) 213–223.
[23] O. Alexeev, G.W. Graham, D.W. Kim, M. Shelef, B.C. Gates, Phys. Chem. Chem. Phys. 1 (1999) 5725–5733.
[24] A. Holmgren, B. Andersson, D. Duprez, Appl. Catal. B 22 (1999) 215–230.
[25] J.A. Anderson, C.H. Rochester, Catal. Today 10 (1991) 275–282.
[26] L. Kustov, W.M.H. Sachtler, J. Mol. Catal. 71 (1992) 233–244.
[27] K. Chakarova, M. Mihaylov, K. Hadjiivanov, Micropor. Mesopor. Mater. 81 (2005) 305–312.
[28] K. Chakarova, M. Mihaylov, K. Hadjiivanov, Catal. Commun. 6 (2005) 466–471.
[29] M. Mihaylov, K. Chakarova, K. Hadjiivanov, O. Marie, M. Daturi, Langmuir 21 (2005) 11821–11828.

[30] V. Zholobenko, G.-D. Lei, B.T. Carvill, B.A. Lenner, W.M.H. Sachtler, J. Chem. Soc., Faraday Trans. 90 (1994) 233–238.
[31] H. Bischoff, G.I. Jaeger, G. Schulz-Ekloff, L. Kubelkova, J. Mol. Catal. 80 (1993) 95–103.
[32] T. Hattori, E. Nagata, Sh. Komai, Y. Murakami, J. Chem. Soc., Chem. Commun. (1986) 1217–1218.
[33] G. Longoni, P. Chini, J. Am. Chem. Soc. 98 (1976) 7225–7231.
[34] L. Kubelkova, J. Vylita, L. Brabec, L. Drozdova, T. Bolom, J. Novakova, G. Schulz-Ekloff, N.I. Jaeger, J. Chem. Soc. Faraday Trans. 92 (1996) 2035–2041.
[35] L. Brabec, J. Mol. Catal. A 169 (2001) 127–136.
[36] M. Beneke, L. Brabec, N. Jaeger, J. Novakova, G. Schulz-Ekloff, J. Mol. Catal. A 157 (2000) 151–161.
[37] J.H. Scofield, J. Electron Spectrosc. Rel. Phenom. 8 (1976) 129–137.
[38] D. Briggs, M.P. Seah, Practical Surface Analysis, vol. 1, 2 ed., Willey & Sons, 1993.
[39] L.R. Raddi de Araujo, M. Schmal, Appl. Catal. A 203 (2000) 275–284.
[40] S. Zafeiratos, G. Papakonstantinou, M.M. Jacksic, S.G. Neophytides, J. Catal. 232 (2005) 127–136.
[41] T.L. Barr, J. Phys. Chem. 82 (1978) 1801–1810.
[42] S.-H. Chien, M.-Ch. Kuo, Ch.-H. Lu, K.-N. Lu, Catal. Today 97 (2004) 121–127.
[43] J.W. Jenkins, B.D. McNicol, S.D. Robertson, Chem. Technol. 7 (1977) 316–319.
[44] I. Sobczak, M. Ziolek, M. Nowacka, Micropor. Mesopor. Mater. 78 (2005) 103–116.
[45] N.W. Hurst, S.J. Gentry, A. Jones, B.D. McNicol, Catal. Rev. Sci. Eng. 24 (1982) 233–309.
[46] B.D. McNicol, J. Catal. 46 (1977) 438–440.
[47] H. Knözinger, S. Huber, J. Chem. Soc. Faraday Trans. 94 (1998) 2047–2059.
[48] O. Cairon, T. Chevreau, J. Chem. Soc. Faraday Trans. 94 (1998) 323–330.
[49] T. Pieplu, F. Poignant, A. Vallet, J. Saussey, J.-C. Lavalley, G. Mabilon, Stud. Surf. Sci. Catal. 96 (1995) 619–629.
[50] K. Hadjiivanov, H. Knözinger, Chem. Phys. Lett. 303 (1999) 513–520.
[51] P. Kubanek, H.-W. Schmidt, B. Spliethoff, F. Schüth, Micropor. Mesopor. Mater. 77 (2005) 89–96.
[52] J.-L. Freysz, J. Saussey, J.-C. Lavalley, P. Bourgesy, J. Catal. 197 (2001) 131–138.
[53] F. Boccuzzi, G. Ghiotti, A. Chiorino, L. Marchese, Surf. Sci. 233 (1990) 141–152.
[54] K. Hadjiivanov, E. Ivanova, D. Klissurski, Catal. Today 70 (2001) 75–84.
[55] M. Mihaylov, K. Hadjiivanov, H. Knözinger, Phys. Chem. Chem. Phys. 8 (2006) 407–417.
[56] R. Ripan, I. Ceteanu, Inorganic Chemistry, Mir, Moscow, 1972.
[57] http://www.webelements.com/webelements/elements/text/periodic-table/radii.html.
[58] P. Gallezot, Molecular Sieves: Preparation of Metal Clusters in Zeolites, vol. 3, Springer-Verlag, Berlin, Heidelberg, 2002.
[59] K. Hadjiivanov, M. Kantcheva, D. Klissurski, J. Chem. Soc., Faraday Trans. 92 (1996) 4595–4600.
[60] S.B. Jang, M.S. Jeong, Y. Kim, S.H. Song, K. Seff, Micropor. Mesopor. Mater. 28 (1999) 173–183.
[61] S. Coluccia, L. Marchese, G. Martra, Micropor. Mesopor. Mater. 30 (1999) 43–56.
[62] K. Hadjiivanov, P. Massiani, H. Knözinger, Phys. Chem. Chem. Phys. 1 (1999) 3831–3838.
[63] K. Hadjiivanov, E. Ivanova, M. Kantcheva, E. Cifitikli, D. Klissurski, L. Dimitrov, H. Knozinger, Catal. Commun. 3 (2002) 313–319.
[64] M.N. Bae, M.K. Song, Y. Kim, K. Seff, Micropor. Mesopor. Mater. 63 (2003) 21–31.